Coherent and incoherent second harmonic generation in planar *G*-shaped nanostructures

E. A. Mamonov,[1,*] T. V. Murzina,[1] I. A. Kolmychek,[1] A. I. Maydykovsky,[1] V. K. Valev,[2] A. V. Silhanek,[3] E. Ponizovskaya,[4] A. Bratkovsky,[4] T. Verbiest,[2] V. V. Moshchalkov,[3] and O. A. Aktsipetrov[1]

[1]*Department of Physics, M.V. Lomonosov Moscow State University, Leninskie Gory, Moscow 119991, Russia*

[2]*Molecular Electronics and Photonics, INPAC, Katholieke Universiteit Leuven, Celestijnenlaan 200 D, B-3001 Leuven, Belgium*

[3]*Nanoscale Superconductivity and Magnetism Pulsed Fields Group, INPAC, Katholieke Universiteit Leuven, Celestijnenlaan 200 D, B-3001 Leuven, Belgium*

[4]*Hewlett-Packard Laboratories, 1501 Page Mill Road, Palo Alto, California 94304, USA*

**Corresponding author: mamonov@shg.ru*

Received June 2, 2011; revised July 13, 2011; accepted July 29, 2011; posted August 24, 2011 (Doc. ID 148635); published September 14, 2011

Azimuthal anisotropy of Stokes parameters of the second harmonic generation (SHG) generated and observed in reflection from a periodic planar area of *G*-shaped gold nanostructures is studied. A strong anisotropy of both coherent and incoherent SHG components is observed. Finite-difference time-domain calculations prove that the observed effects are due to the anisotropic enhancement of the fundamental radiation within the *G*-shaped structures. © 2011 Optical Society of America

OCIS codes: 190.2620, 230.5298, 290.5820, 260.2710.

Optical metamaterials are artificial nanostructured systems that exhibit certain optical properties not present in the native materials [1,2]. It has been demonstrated that a number of new effects with possible application in nanophotonic devices such as anomalous transmission [3] and negative refraction [4] can be observed in planar metamaterials. Several two-dimensional periodic templates have been examined: fishnet [5], *T*- and *L*-shaped [6,7], gammadions [8], *bow-tie* structures [9], etc. It has been proven that the geometrical shape of a particular structure determines a specific distribution of the local optical field in it, as well as the conditions for the plasmon excitation. Additional functional properties can arise in chiral metamaterials, where effects so far only observed in three-dimensional media, such as polarization plane rotation [8,10] and asymmetric propagation of electromagnetic waves [11], can be revealed.

Nonlinear optical studies of metamaterials performed over the last few years have been mostly concentrated on second harmonic generation (SHG). The SHG technique is known to be extremely sensitive to the local optical field distributions as well as to the symmetry of nanoobjects [12,13]. It is precisely the latter property that has made SHG a promising technique for revealing novel phenomena in the field of optical response of metamaterials [14]. For instance, asymmetric SHG was observed in chiral macroscopically symmetric *G*-shaped structures [15,16]. Pronounced SHG azimuthal anisotropic dependencies were observed for structures of different chirality, i.e., composed of *G* and mirror-*G* enantiomers. In other words, it was proven that the chirality of a single nanostructure determines the symmetry of the SHG anisotropy. The observed effects were attributed to different structural conditions for the local surface plasmon excitation in mirror enantiomers and to the lighting rod effect. Up to now, however, a detailed investigation of the coherence of the nonlinear optical response of planar metamaterials is still lacking. In this Letter the anisotropy of the Stokes parameters of the SHG generated and observed in reflection from planar *G*-shaped metamaterials is presented. The studies are performed for linearly polarized fundamental radiation. Stokes parameters at the SHG frequency are deconvoluted from the anisotropy and polarization measurements of the SHG response. The discussion of the experimental results is supported by calculations of the optical field distribution in the *G*-shaped structures.

The sample consists of a periodic array of *G*-shaped nanostructures made of a 25 nm thick Au film deposited onto a Si(100) substrate with a 200 nm thick SiO_2 layer. The line width and the separation between the neighboring *G* structures is 200 nm; the diagram of a single *G* element, along with the sizes and the experimental geometry, is shown in the inset of Fig. 1. The sample fabrication procedure is described in more detail in [16,17].

For the SHG experiments we used the output of a Ti:sapphire laser at 780 nm with a repetition frequency of 80 MHz. The pulse duration was 80 fs, and the mean power was 150 mW. The pump radiation was focused on the sample into a spot of 50 μm in diameter at an angle of incidence of 45°. Reflected SHG radiation was spectrally selected by BG39 Schott color filters, passed through a diaphragm with an aperture of 10°, and detected by a photomultiplier. The pump beam polarization was controlled by a $\lambda/2$ plate, and the SHG polarization was detected by a Babinet–Soleil compensator and a polarizer.

Figure 1 shows the dependence of the SHG intensity, $I_{2\omega}$, on the azimuthal angle of the sample, ψ, measured for different combinations of polarizations of the fundamental and SHG waves. All the $I_{2\omega}(\psi)$ dependencies reveal four maxima, and those measured for *p*- and *s*-polarized pump radiation are shifted in phase by $\pi/4$ with respect to each other. This fact proves that the observed SHG anisotropy is determined by the polarization of the fundamental beam. It should be noted that nonzero $I_{2\omega}$ values observed in the azimuthal minima of the *s*-polarized SHG indicate the existence of an isotropic

 © 2011 Optical Society of America

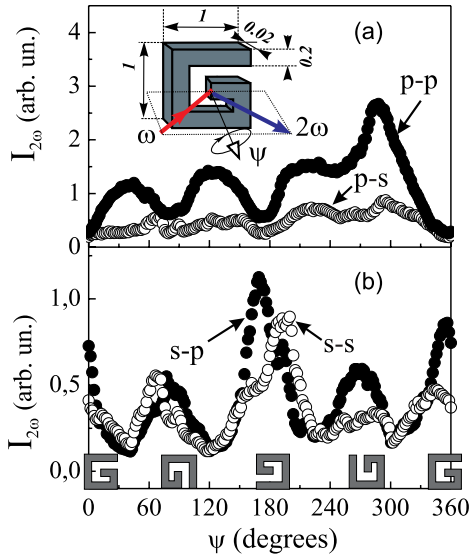

Fig. 1. (Color online) (a), (b) SHG anisotropy for *p*-*p*, *p*-*s*, *s*-*p*, and *s*-*s* combinations of polarizations of the fundamental and SHG waves denoted by the first and second letters, respectively; *p* denotes polarization parallel to the plane of incidence, and *s*, perpendicular to it. Inset: a schematic view of the structure and the plane of incidence for $\psi = 0°$; the indicated dimensions are in micrometers. The orientation of the *G*-elements at $\psi = 0°$, 90°, 180°, 270°, and 360° are shown below the experimental data; the plane of incidence corresponds to $\psi = 0$.

s-polarized SHG, that is forbidden for periodic structures and should be attributed to an incoherent, i.e., dephased and diffusely scattered, SHG [18]. The inset in Fig. 2(a) shows the SHG scattering indicatrix, i.e., the $I_{2\omega}$ dependence on the polar angle of scattering, $I_{2\omega}(\theta)$, measured for the azimuthal angle $\psi = 0$. A pronounced specular SHG peak is observed at $\theta = 90°$ that corresponds to the generation of a coherent (polarized and specular) light [18]. At the same time, a nonzero diffuse SHG detected

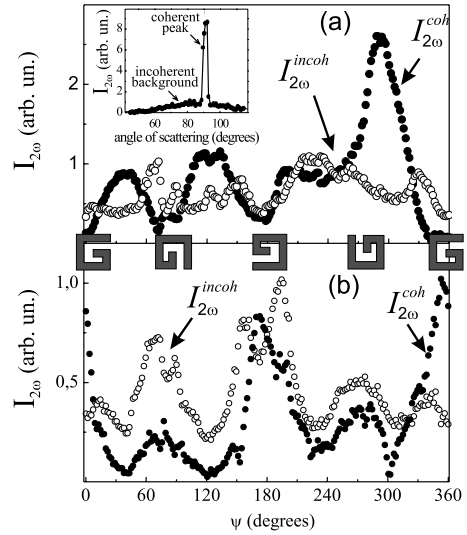

Fig. 2. Azimuthal dependencies of coherent (filled circles) and incoherent (open circles) SHG under excitation by (a) *p*-polarized and (b) *s*-polarized fundamental beams. Inset: the SHG indicatrix measured for $\psi = 0°$ and *p*-ω, *p*-2ω combination of polarizations.

in a wide scattering range indicates the presence of an incoherent SHG.

For a full characterization of the polarization of the reflected SHG, we measured the azimuthal dependencies of the *p*, *s*, +45°, and −45° linearly polarized SHG, together with the left- and right-hand circularly polarized SHG components. In all cases, the fundamental beam was linearly polarized. These measurements allowed us to estimate the anisotropic dependencies of the Stokes parameters, S_0, S_1, S_2, and S_3, where S_0 corresponds to the total SHG intensity, $S_1 = I_{2\omega}^{p} - I_{2\omega}^{s}$, $S_2 = I_{2\omega}^{+45°} - I_{2\omega}^{-45°}$, $S_3 = I_{2\omega}^{\text{right}} - I_{2\omega}^{\text{left}}$, and the superscripts denote the SHG polarization [19]. Azimuthal dependencies of both polarized, i.e., coherent, $I_{2\omega}^{\text{coh}}$ and depolarized, i.e., incoherent, $I_{2\omega}^{\text{incoh}}$ SHG components are shown in Fig. 2. These components were calculated as $I_{2\omega}^{\text{coh}} = \sqrt{S_1^2 + S_2^2 + S_3^2}$ and $I_{2\omega}^{\text{incoh}} = S_0 - I_{2\omega}^{\text{coh}}$, correspondingly. It can be seen that $I_{2\omega}^{\text{coh}}$ and $I_{2\omega}^{\text{incoh}}$ are comparable and reveal a very similar type of azimuthal dependence. The obtained results show that the anisotropy of the SHG response from *G*-shaped nanostructures is due to the anisotropy of the local field distribution. Both $I_{2\omega}^{\text{coh}}$ and $I_{2\omega}^{\text{incoh}}$ are amplified for a certain orientation of the sample with respect to the polarization plane of the pump beam. This amplification is most likely due to the field enhancement achieved for certain azimuthal positions of the sample. This assumption will be confirmed below by numerical calculations.

In order to reveal the role of the local field in the SHG anisotropy, the field distribution in *G*-shaped nanostructures was calculated for the fundamental and SHG wavelengths. The commercial software package FDTD Solutions (Lumerical Solutions, Inc., Canada) was used. For the simulations, the structural parameters of the *G*-elements and the geometry of interaction were identical to those in the experiment; boundary conditions were periodic, and the substrate was not taken into account. Further simulations have affirmed that the presence of the substrate does not influence the field distribution. The pump and SHG fields were calculated, as both of them determine the SHG intensity: $I_{2\omega} \propto \langle(\hat{\chi}^{(2)} L_{2\omega}(\psi) L_{\omega}^2(\psi))^2\rangle I_{\omega}^2$, where L_{ω} and $L_{2\omega}$ are local field factors at the corresponding wavelengths, I_{ω} is the pump intensity, and the brackets denote the statistical averaging over the laser spot area.

Figure 3 shows the distribution of L_{ω} and $L_{2\omega}$ within the *G*-shaped elements. Two azimuthal orientations of the *p*-polarized field were considered, $\psi = 0°$ and 45°. It can be seen that L_{ω} is strongly inhomogeneous and the field localization in the structure is changed significantly for different ψ angles. The distribution of $L_{2\omega}$ within the structure is less pronounced; this may be due to a high absorption of gold *G*-shaped nanostructures at the SHG wavelength of 400 nm, which corresponds to previously obtained results [15]. It should be noted that the scale in the bottom panels is much smaller as compared with the upper ones. Taking into consideration a strong difference in the degree of localization of the fundamental and SHG fields, together with the fourth power dependence of $I_{2\omega}$ on L_{ω}, we conclude that the SHG anisotropy is due to the azimuthal enhancement of $L_{\omega}(\psi)$. To support this conclusion, an estimation of the $I_{2\omega}$ changes for the azimuthal

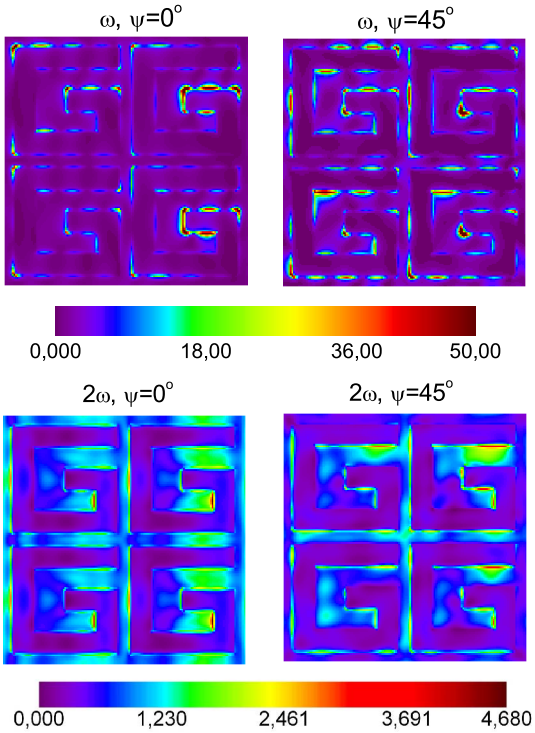

Fig. 3. (Color online) Local field distribution of the p-polarized fundamental (top panels) and SHG (bottom panels) radiation for the azimuthal positions of the samples $\psi = 0°$ (left panels) and $\psi = 45°$ (right panels).

orientations of the sample $\psi = 180°$ and 290° was made. These ψ values correspond to the minimum and maximum of the coherent p-polarized SHG [see Fig. 2(a)]. The experiment gives the ratio of the total SHG intensity as $\frac{I_{2\omega}(290°)}{I_{2\omega}(180°)} \approx 4.5$, which is in agreement with the numerically calculated ratio for the averaged local field factors, $(\frac{\langle\langle L_\omega(290°)\rangle\rangle}{\langle\langle L_\omega(180°)\rangle\rangle})^4 \approx 5$ [Fig. 1(a)].

In conclusion, azimuthal anisotropy of the Stokes parameters of the SHG reflected from a periodic planar array of G-shaped nanostructures was studied. Anisotropic enhancement of both coherent and incoherent SHG components was observed. Numerical calculations of the spatial local field factor distribution at the fundamental and SHG wavelengths have shown that the anisotropy of the averaged field factor of the pump radiation is responsible for the observed effects.

T. Verbiest and V. V. Moshchalkov acknowledge financial support from the Fund for Scientific Research—Flanders (FWO-V), the Katholieke Universiteit Leuven (GOA), Methusalem Funding by the Flemish government, and the Belgian Interuniversity Attraction Poles (IAP) Programme. V. K. Valev and A. V. Silhanek are grateful for the support from the FWO-V. The financial support from Russian Foundation for Basic Research (RFBR) grants 11-02-01289 and 10-02-00967 is greatly acknowledged.

References

1. J. B. Pendry, Contemp. Phys. **45**, 191 (2004).
2. V. Shalaev, Nat. Photon. **1**, 41 (2007).
3. J. A. H. van Nieuwstadt, M. Sandtke, R. H. Harmsen, F. B. Segerink, J. C. Prangsma, S. Enoch, and L. Kuipers, Phys. Rev. Lett. **97**, 146102 (2006).
4. E. Kim, Y. R. Shen, W. Wu, E. Ponizovskaya, Z. Yu, A. M. Bratkovsky, S.-Y.Wang, and R. S. Williams, Appl. Phys. Lett. **91**, 173105 (2007).
5. Z. Wei, Y. Cao, J. Han, C. Wu, Y. Fan, and H. Li, Appl. Phys. Lett. **97**, 141901 (2010).
6. H. Husu, B. K. Canfield, J. Laukkanen, B. Bai, M. Kuittinen, J. Turunen, and M. Kauranen, Metamaterials **2**, 155 (2008).
7. S. Kujala, B. K. Canfield, M. Kauranen, Y. Svirko, and J. Turunen, Opt. Express **16**, 17196 (2008).
8. A. Papakostas, A. Potts, D. M. Bagnall, S. L. Prosvirnin, H. J. Coles, and N. I. Zheludev, Phys. Rev. Lett. **90**, 107404 (2003).
9. S. Kim, J. Jin, Y.-J. Kim, I.-Y. Park, Y. Kim, and S.-W. Kim, Nature **453**, 757 (2008).
10. V. A. Fedotov, A. S. Schwanecke N. I. Zheludev, V. V. Khardikov, and S. L. Prosvirnin, Nano Lett. **7**, 1996 (2007).
11. V. A. Fedotov, P. L. Mladyonov, S. L. Prosvirnin, A. V. Rogacheva, Y. Chen, and N. I. Zheludev, Phys. Rev. Lett. **97**, 167401 (2006).
12. O. A. Aktsipetrov, T. V. Murzina, and E. M. Kim, R. V. Kapra, A. A. Fedyanin, M. Inoue, A. F. Kravets, S. V. Kuznetsova, M. V. Ivanchenko, and V. G. Lifshits, J. Opt. Soc. Am. B **22**, 138 (2005).
13. C. Hubert, L. Billot, P.-M. Adam, R. Bachelot, P. Royer, J. Grand, D. Gindre, K. D. Dorkenoo, and A. Fort, Appl. Phys. Lett. **90**, 181105 (2007).
14. M. W. Klein, M. Wegener, N. Feth, and S. Linden, Opt. Express **15**, 5238 (2007).
15. V. K. Valev, A. V. Silhanek, N. Verellen, W. Gillijns, P. Van Dorpe, O. A. Aktsipetrov, G. A. E. Vandenbosch, V. V. Moshchalkov, and T. Verbiest, Phys. Rev. Lett. **104**, 127401 (2010).
16. V. K. Valev, X. Zheng, C. G. Biris, A. V. Silhanek, V. Volskiy, B. De Clercq, O. A. Aktsipetrov, M. Ameloot, N. C. Panoiu, G. A. E. Vandenbosch, and V. V. Moshchalkov, Opt. Mater. Express **1**, 36 (2011).
17. V. K. Valev, N. Smisdom, A. V. Silhanek, B. De Clercq, W. Gillijns, M. Ameloot, V. V. Moshchalkov, and T. Verbiest, Nano Lett. **9**, 3945 (2009).
18. O. A. Aktsipetrov, I. M. Baranova, and Yu. A. Il'inskii, Sov. Phys. JETP **64**, 167 (1986).
19. S.-M. F. Nee, in *The Measurement, Instrumentation and Sensors Handbook*, J. G. Webster, ed. (CRC, 1999), pp. 60-1–60-24.